

Progressive attenuation of the longitudinal kinetics in the common carotid artery: preliminary *in vivo* assessment

Guillaume Zahnd^{a,*}, Simone Balocco^{b,c}, André Sérusclat^d, Philippe Moulin^{e,f},
Maciej Orkisz^g, Didier Vray^g

^a*Biomedical Imaging Group Rotterdam, Departments of Radiology and Medical Informatics, Erasmus MC, Rotterdam, The Netherlands*

^b*Department of Applied Mathematics and Analysis, University of Barcelona, Barcelona, Spain*

^c*Computer Vision Center, Barcelona, Spain*

^d*Department of Radiology, Louis Pradel Hospital, Lyon, France*

^e*Department of Endocrinology, Louis Pradel Hospital, Hospices Civils de Lyon, Université Lyon 1, Lyon, France*

^f*INSERM UMR 1060, Lyon, France*

^g*Université de Lyon, CREATIS; CNRS UMR 5220; INSERM U1044; INSA-Lyon; Université Lyon 1; France*

Abstract

Longitudinal kinetics (LOKI) of the arterial wall consists in the shearing motion of the intima-media complex over the adventitia layer in the direction parallel to the blood flow during the cardiac cycle. The aim of this study is to investigate the local variability of LOKI amplitude along the length of the vessel. Using a previously validated motion-estimation framework, 35 *in vivo* longitudinal B-mode ultrasound cine-loops of healthy common carotid arteries were analyzed. Results demonstrate that LOKI amplitude is progressively attenuated along the length of the artery, as it is larger in regions located on the proximal side of the image (*i.e.* toward the heart), and smaller in regions located on the distal side

*Corresponding Author: g.zahnd@erasmusmc.nl

Manuscript published in *Ultrasound in Medicine and Biology* (DOI: doi:10.1016/j.ultrasmedbio.2014.07.019). The final version of the paper is available at: <http://dx.doi.org/10.1016/j.ultrasmedbio.2014.07.019>

of the image (*i.e.* toward the head), with an average attenuation coefficient of $-2.5 \pm 2.0 \text{ \%} \cdot \text{mm}^{-1}$. Reported for the first time in this study, this phenomenon is likely to be of great importance for improved understanding of atherosclerosis mechanisms, and has potential to constitute a novel index of arterial stiffness.

Keywords: Longitudinal kinetics, Ultrasound imaging, Common carotid artery, Motion tracking, Atherosclerosis, Arterial stiffness

1 Introduction

2 Cardiovascular diseases represent the leading cause of human mortality and
3 morbidity (WHO, 2013). To assess cardiovascular risk, the common carotid artery
4 (CCA) has been extensively analyzed *in vivo* using B-mode ultrasound (US) imag-
5 ing. A few pioneering studies have investigated the deformation of the arterial wall
6 tissues in the direction parallel to the blood flow during the cardiac cycle (Persson
7 et al., 2003). This phenomenon, hereafter referred to as “*longitudinal kinetics*”
8 (LOKI), corresponds to the cyclic shearing motion of the intima-media complex
9 with respect to the tunica adventitia (Figure 1).

10 Recent findings contributed to elucidate the association between LOKI and
11 vascular pathophysiology. Namely, LOKI has been reported to induce a wall shear
12 strain (WSS) reflecting arterial stiffness (Cinthio et al., 2006; Nilsson et al., 2010;
13 Zahnd et al., 2011b; Idzenga et al., 2012b), and has been associated with the
14 presence of cardiovascular risk factors (Ahlgren et al., 2009; Zahnd et al., 2011a,
15 2012; Ahlgren et al., 2012) as well as with atherosclerotic plaque burden (Sved-
16 lund and Gan, 2011; Soleimani et al., 2012; Gastouniotti et al., 2013). Also, it
17 was reported to predict 1-year cardiovascular outcome in patients with suspected
18 coronary artery disease (Svedlund et al., 2011). These findings strongly suggest

19 that LOKI constitutes a solid candidate to become a novel valuable image-based
20 biomarker for improved cardiovascular risk prediction.

21 Various advanced techniques have been proposed to evaluate LOKI in B-
22 mode US cine-loops. An echo-tracking approach, based on a careful imaging
23 protocol to track a tiny region of interest (ROI) encompassing a well contrasted
24 speckle pattern, provided a detailed characterization of LOKI (Cinthio et al., 2005).
25 Towards accurate LOKI evaluation in routinely-acquired data, robust motion-
26 tracking approaches have been proposed, based on Kalman filtering (Gastouni-
27 oti et al., 2011; Zahnd et al., 2013), weighted least-squares optical flow (Golemati
28 et al., 2012), and finite impulse response filtering (Gastounioti et al., 2013). Radio-
29 frequency US was also used to assess the wall shear strain by means of a coarse-
30 to-fine cross-correlation based strain algorithm (Idzenga et al., 2012a).

31 One of the main parameters derived from LOKI analysis is its maximal peak-
32 to-peak amplitude ΔX , (*i.e.* the total amplitude of the longitudinal motion of
33 the intima and media layers along the direction parallel to the blood flow), which
34 is significantly reduced in patients with presumably stiffer arteries (Zahnd et al.,
35 2011a; Svedlund et al., 2011; Zahnd et al., 2012). Yet, the influence of the loca-
36 tion of the assessed ROI onto the resulting motion amplitude ΔX is still unclear.
37 Indeed, it has previously been reported by our team that different resulting tra-
38 jectories could be observed when tracking points in different regions (*i.e.* on the
39 right, center, and left side of the image) (Zahnd et al., 2011a).

40 The aim of this pilot study is to characterize such local variability of LOKI
41 amplitude ΔX in longitudinal B-mode US cine-loops of *in vivo* healthy CCA. For
42 each cine-loop analyzed, the motion of the far wall at different locations within
43 the intima-media complex is evaluated on a collection of points by means of ro-

44 bust speckle tracking, using a previously validated framework (Zahnd et al., 2013).
45 Our rationale is the following: mechanical LOKI-inducing forces are likely to be
46 progressively dissipated along the propagation in the artery, reflecting the elas-
47 tic damping role of the circulatory system. Therefore, it is expected that ΔX is
48 systematically lower in ROIs located on the “*distal*” side of the image (*i.e.* to-
49 ward the head) compared to ROIs located on the “*proximal*” side (*i.e.* toward
50 the heart). To the best of our knowledge, this phenomenon has not previously be
51 observed *in vivo*.

52 **Methods**

53 *Study population*

54 Fifty-seven healthy volunteers (mean age: 37.9 ± 14.1 y.o., 24 males) have been
55 involved in this study. All participants were cardiovascular risk factor-free (tobacco
56 use, hypercholesterolemia, diabetes, hypertension, or particular family history), as
57 assessed by an oral questionnaire. Written informed consent was obtained from
58 all participants. The study fulfilled the requirements of our institutional review
59 board and the ethics committee.

60 *Acquisition of carotid artery ultrasound sequences*

61 The image acquisition protocol has been previously described (Zahnd et al.,
62 2013). Briefly, longitudinal B-mode US cine-loops of the left CCA were obtained
63 using a clinical scanner (Antares, Siemens Erlangen), equipped with a 7.5- to 10-
64 MHz linear array transducer. Acquisition was performed by an expert physician
65 during at least two full cardiac cycles, with the probe centered approximately
66 2 cm from the carotid bifurcation. The probe was systematically oriented in such

67 way that the left border of the image corresponded to the distal side, and the
68 right border to the proximal side, as pictured in Figure 1a. To avoid out-of-plane
69 motion artifacts, specific care was taken to position the probe in the longitudinal
70 plane of the vessel. The frame rate was 26 fps, and the width of the acquired US
71 image was 26 mm, with a pixel size in both longitudinal and radial directions was
72 30 μm .

73 *Quantification of LOKI amplitude ΔX*

74 For each participant, a collection of salient points located within the intima-
75 media complex of the far wall were manually selected to be tracked (Fig. 2a). Such
76 salient echo scatterers are defined as well contrasted speckle patterns that remain
77 clearly perceptible during the entire cine-loop (Cinthio et al., 2005; Zahnd et al.,
78 2013). In order to assess the local variability of LOKI, motion tracking has to
79 be performed on at least two different sites in the image. Therefore, participants
80 presenting either none or only one salient echo were rejected from the study. For
81 all remaining participants, the bi-dimensional (2D, *i.e.* radial and longitudinal)
82 temporal trajectory of each salient echo during the entire cine-loop was extracted,
83 using a framework previously developed and validated by our team (Zahnd et al.,
84 2013). Finally, LOKI amplitude ΔX was measured from the resulting trajectory
85 of each tracked point. The amplitude ΔX was determined as the peak-to-peak
86 amplitude of the longitudinal component of the 2D trajectory, averaged over two
87 cardiac cycles (Fig. 2b).

88 *Attenuation coefficient Z*

89 We define the attenuation coefficient Z as the slope of the linear regression that
90 fits, for a given cine-loop, the set of points whose x -coordinate is the distance X

91 from the right border of the image, and whose y -coordinate is the corresponding
92 measured amplitude ΔX (Fig. 2c).

93 *Statistical analysis*

94 The Pearson's correlation coefficient R was used to evaluate the correlation
95 between LOKI amplitude ΔX and the attenuation coefficient Z . Statistical analysis
96 was performed using MATLAB (MATLAB 7.13, The MathWorks Inc., Natick,
97 MA, USA, 2011).

98 **Results**

99 For each participant, at least one salient point could be observed. Twenty-
100 two participants were rejected from the study, as they presented only a single
101 salient point to be tracked. In the remaining 35 participants, the average number
102 of tracked points was 3.7 ± 1.5 (the number of cine-loops presenting 2, 3, 4, 5,
103 6, and 7 measurement points was 9, 9, 7, 5, 3, and 2, respectively). For those
104 analyzed participants, the average width of the total assessed region, defined as
105 the distance between the two extreme proximal and distal measurement points,
106 was 15.3 ± 5.4 mm (range: [3.2, 25.1] mm), corresponding to 56 ± 19 % of the
107 entire image width, which was 26 mm. Within the analyzed region, the average
108 distance between two neighbor measurement points was 5.3 ± 3.6 mm (range:
109 [1.0, 18.7] mm).

110 The average LOKI amplitude ΔX of all individual tracked points was $722 \pm$
111 284 μm . As the number of tracked points is subject-dependent, we also define $\widehat{\Delta X}$
112 as the mean value of all ΔX measurements for a given participant. The average
113 amplitude $\widehat{\Delta X}$ for all participants was 717 ± 260 μm . For the majority of the

114 analyzed subjects (*i.e.* 33 out of 35), we made the following observation: LOKI
115 amplitude ΔX is systematically larger for points located on the proximal side of the
116 image, and smaller for points located on the distal side of the image, as depicted
117 in Figure 2a,b.

118 Examples of the attenuation coefficient Z estimated in different participants
119 are displayed in Figure 3. Calculating the average attenuation coefficient Z of all
120 35 participants, we confirmed the presence of a progressive attenuation of LOKI
121 amplitude towards the distal direction, with an average Z value of $-17 \pm 16 \mu\text{m} \cdot$
122 mm^{-1} (range $[-91, 17] \mu\text{m} \cdot \text{mm}^{-1}$, as displayed in Figure 4. This attenuation can
123 also be quantified as follow: within a given CCA segment, the motion between two
124 points separated by 1 mm undergoes a decrease corresponding to $-2.5 \pm 2.0 \%$
125 of the average LOKI amplitude $\widehat{\Delta X}$ of the vessel. Arteries with a larger LOKI
126 amplitude were not found to also undergo a stronger attenuation, as no significant
127 correlation could be observed between the mean LOKI amplitude per subject $\widehat{\Delta X}$
128 and the corresponding attenuation coefficient Z ($R=0.22$).

129 The average dispersion error with respect to the linear regression model (*i.e.* the
130 mean absolute vertical distance between the estimated points and the regression
131 line) as a function of the number of tracked points is displayed in Table 1. The
132 overall average absolute error of fitting between all the measurement points and
133 the linear regression model was $34 \pm 36 \mu\text{m}$. By definition, the dispersion error
134 generated by linear regression is null in cine-loops with exactly 2 tracked points.
135 For this reason, we also calculated the average absolute error of fitting in cine-loops
136 with at least 3 measurement points, which was $39 \pm 36 \mu\text{m}$. Such dispersion remains
137 small in comparison with the average LOKI amplitude $\widehat{\Delta X}$ (*i.e.* $717 \pm 260 \mu\text{m}$), as
138 depicted in Figure 3. The dispersion was also nearly two times smaller than the

139 tracking accuracy of the present framework in the longitudinal direction, previously
140 validated in (Zahnd et al., 2013). Indeed, with respect to the reference that was
141 generated from the manual tracings of three experienced observers, the average
142 absolute error of the present framework for ΔX quantification was $74 \pm 68 \mu\text{m}$,
143 while the inter- and intra-observer variability was $79 \pm 103 \mu\text{m}$ and $62 \pm 103 \mu\text{m}$,
144 respectively.

145 Discussion

146 The principal finding of this study is the presence of a systematic local variabil-
147 ity of LOKI amplitude ΔX , and more specifically a decreasing trend in ΔX within
148 the imaged region (Fig. 2). That is to say, intima and media tissues located on
149 the proximal side of the image (*i.e.* towards the heart, right border of the image)
150 present an overall larger motion amplitude than tissues located on the distal side
151 (*i.e.* towards the head, left border of the image). This breakthrough suggests that
152 LOKI-inducing forces are progressively attenuated as they further propagate from
153 the heart to peripheral organs. To the best of our knowledge, the present study is
154 the first to report this finding.

155 LOKI amplitude ΔX was assessed *in vivo* at several (at least two) locations
156 of the CCA in 35 healthy volunteers. Fitting the measured amplitudes with lin-
157 ear regression, we observed an average attenuation coefficient Z equal to $-17 \pm$
158 $16 \mu\text{m}/\text{mm}$ (Fig. 4), which corroborates the presence of a decreasing trend along
159 the arterial length. We observed an increase of the fitting error with the number
160 of measurement points. This can be explained by the fact that a larger amount
161 of roughly aligned points would increase the average distance between each point
162 and its vertical projection on the linear regression.

163 To perform the measurements, we used a Kalman-based tracking framework,
164 previously developed by our team and validated on a dataset of 82 subjects (Zahnd
165 et al., 2013). The average absolute dispersion error of the measured amplitudes ΔX
166 against a linear regression model was roughly two times smaller than the previously
167 validated *i)* tracking accuracy of the present framework, and *ii)* inter- and intra-
168 observer variability. This strengthens the validity of the observed negative trend
169 in ΔX across the width of the imaged regions.

170 This study implies a major caveat that should be taken into account when inves-
171 tigating LOKI in future work. This recommendation concerns the quantification
172 of LOKI amplitude ΔX (*i.e.* the quantity of tissue deformation in the longitudinal
173 direction) in a given subject. This parameter is relevant, as previous studies have
174 demonstrated a negative association between ΔX and the presence of cardiovas-
175 cular risk factors (Zahnd et al., 2011a; Svedlund et al., 2011; Zahnd et al., 2012;
176 Ahlgren et al., 2012; Golemati et al., 2012; Gastounioti et al., 2013). Due to the
177 attenuation phenomenon described in this study, LOKI amplitude ΔX is depen-
178 dent on the initial location of the tracked point, and is thus subject to variability
179 within the imaged region. Therefore, to thoroughly assess ΔX in a cine-loop, it
180 would be more insightful to systematically evaluate LOKI at a calibrated location.
181 From our experience however, a standardized horizontal reference coordinate can-
182 not be fixed to determine the point to be tracked for the entire dataset, due to
183 a variability in image local quality between different cine-loops. An alternative
184 solution could be to evaluate LOKI in a set of different locations where the image
185 quality is optimal, in the aim to determine the average value $\widehat{\Delta X}$.

186 The attenuation phenomenon observed in this study can be explained by a num-
187 ber of factors contributing to arterial fixation *via* tethering to surrounding tissues:

188 *i)* side branches, *ii)* perivascular connective tissues, *iii)* vessel three-dimensional
189 tortuosity (Nichols and O'Rourke, 2005). Furthermore, LOKI attenuation can
190 also be explained by the fact that arterial tissues have viscoelastic properties and
191 play a cushioning function to dissipate high blood pressure provoked by pulsatile
192 flow (Benetos et al., 1997). Such damping properties are likely to be associated
193 with wall shear strain, which plays a fundamental role in vasa vasorum circulation
194 as well as endothelial function (Cunningham and Gotlieb, 2004; Chatzizisis et al.,
195 2007).

196 The question of characterizing the actual forces at the origin of LOKI is still
197 unanswered at the moment. Blood friction, creating a tangential force at the
198 surface of the wall, is unlikely to constitute a significant contribution to LOKI.
199 Instead, it is hypothesized that LOKI is induced by a large retrograde wall motion
200 (*i.e.* in the direction opposite to blood flow), provoked by the apical traction of the
201 aortic valve annulus in late systole (Cinthio et al., 2006). The subsequent antegrade
202 motion (*i.e.* in the same direction as the blood flow) is likely to be provoked by
203 the radial systolic stretching caused by the blood volume influx. The amplitude
204 of the pulling force corresponding to the aortic traction, referred to as tricuspid
205 annular plane systolic excursion, was measured in echocardiography and reported
206 to be superior to 17 mm in healthy subjects (Tamborini et al., 2007; Rudski et al.,
207 2010). Accordingly, as the average LOKI amplitude $\widehat{\Delta X}$ in the CCA was found
208 to correspond to $717 \pm 260 \mu\text{m}$, the initial pulling force is likely to be dissipated
209 along the way, which is confirmed by the results of this study. We formulate the
210 hypothesis that LOKI would eventually become null (*viz.*: $\Delta X \approx 0$) at the point
211 where the internal carotid artery enters the skull *via* the carotid canal, through
212 the petrous portion of the temporal bone.

213 Although LOKI amplitude ΔX is associated with cardiovascular risk factors (Zahnd
214 et al., 2011a; Svedlund et al., 2011; Zahnd et al., 2012; Ahlgren et al., 2012;
215 Golemati et al., 2012; Gastounioti et al., 2013), the actual clinical relevance of the
216 attenuation coefficient Z remains to be investigated. Since this pilot study involved
217 healthy middle-aged participants, it is still unclear whether the measured LOKI
218 attenuation coefficient Z reflects vascular health. Future studies, involving patients
219 at cardiovascular risk, are necessary to investigate the association between Z and
220 cardiovascular risk factors (*e.g.* diabetes, hypertension, metabolic syndrome, to-
221 bacco use, age). Further work, focusing on the association between the attenuation
222 coefficient Z and surrogate markers of atherosclerosis (*e.g.* LOKI amplitude ΔX ,
223 intima-media thickness, cross-sectional distensibility, pulse wave velocity), would
224 determine whether Z actually constitutes a reliable and independent biomarker
225 of vascular health. Besides, *in vivo* measurement of the attenuation coefficient Z
226 would enable tissue stiffness to be quantified *via* a patient-specific biomechanical
227 model.

228 This study does present several limitations that open the field to multiple
229 perspectives. First, the present framework requires the presence of several (at least
230 two) bright echo scatterers in the intima-media complex, to accurately track the
231 wall motion during the cardiac cycle and quantify the attenuation coefficient Z . For
232 this reason, 22 subjects out of 57 were rejected from the study as they did not meet
233 this condition. Second, LOKI was approximated by considering the projection of
234 the motion along the horizontal axis. We made the assumption that, since the
235 curvature of the vessel is small in comparison to the amplitude of the wall motion,
236 the radial component of LOKI is negligible. A more accurate evaluation of LOKI
237 could be realized by taking into account the local curvature of the wall to assess the

238 actual tissue motion. This issue will be investigated in future work. Third, we have
239 made the approximation that the variation of ΔX was linear within the imaged
240 region. However, the actual attenuation is most likely to be non-linear along
241 the total arterial tree. Further studies, involving data acquired both upstream
242 (*i.e.* aortic valve annulus) and downstream (*i.e.* carotid bulb, as well as internal and
243 external carotids), would provide valuable information about the local attenuation
244 coefficient Z along the vascular tree. Finally, we have focused on the analysis of
245 the left CCA, which is directly connected to the aorta. It would be insightful to
246 realize a comparison with results obtained on the right CCA, which is connected to
247 the aorta *via* the S-shaped brachiocephalic trunk. Accordingly, the initial pulling
248 force is likely to be further attenuated in the right CCA, and could potentially be
249 reflected by smaller LOKI amplitude ΔX and attenuation coefficient Z . Extending
250 the scope of investigation to other main arteries (*e.g.* popliteal, humeral) would
251 also benefit to a more comprehensive analysis.

252 **Conclusion**

253 In this pilot study, we analyzed B-mode US cine-loops of healthy CCA to
254 assess the local variability of LOKI amplitude ΔX (*i.e.* the quantity of tissue de-
255 formation parallel to the blood flow) within the imaged region during the cardiac
256 cycle. We observed that LOKI amplitude ΔX does undergo a progressive atten-
257 uation along the arterial segment, namely ΔX is larger on the proximal side of
258 the image, and smaller on the distal side, with an average attenuation coefficient
259 of $-2.5 \pm 2.0 \text{ \%} \cdot \text{mm}^{-1}$. To the best of our knowledge, the observation of this
260 phenomenon *in vivo* has not previously been reported. We hypothesize that this
261 gradual decrease reflects a damping role in the circulatory system, and could po-

262 tentially be associated with cardiovascular risk. Further studies are required to
263 investigate this finding.

264 **Figure captions**

265 **Figure 1:** Common carotid artery (CCA). (a) Longitudinal B-mode ultrasound
266 image of a healthy CCA *in vivo*. The direction of the blood flow in the
267 lumen is indicated by the white arrow. (b) Illustration of the longitudinal
268 kinetics (LOKI), occurring within the concentric layers of the wall during
269 the heart beat. Please note that the tissue motion obeys a multiphasic
270 and bidirectional pattern, towards both retrograde and antegrade directions
271 during the cardiac cycle.

272 **Figure 2:** Example of LOKI amplitude ΔX , evaluated on a healthy subject.
273 (a) Location of three regions of interest (ROIs), encompassing the tracked
274 points within the intima-media complex of the far wall. The resulting LOKI
275 amplitude ΔX during the cine-loop is represented by the double arrows.
276 (b) Longitudinal component of the estimated trajectory, for the left (dot-
277 ted red), middle (dashed green), and right (solid blue) tracked points. The
278 peak-to-peak amplitude ΔX of each tracked point is represented by the ver-
279 tical bar of the corresponding color. (c) Representation of the attenuation
280 coefficient Z for this specific cine-loop, determined by linear regression (solid
281 line) of the three tracked points (circles). For each tracked point, the x -
282 and y -coordinates correspond to the abscissa of the ROI in (a), and to the
283 estimated amplitude ΔX in (b), respectively.

284 **Figure 3:** Examples of the attenuation coefficient Z in six participants, evalu-
285 ated by means of linear regression (solid line) of the estimated LOKI am-
286 plitude ΔX (circles) over the length of the imaged region. The x -axis is
287 oriented accordingly to the blood flow direction, from the right border of the

288 image ($x = 0$) towards the left border. The fitting error (err) is indicated,
289 and the corresponding standard deviation is represented by the dashed lines.
290 (a-e) Representative examples of a progressive attenuation of ΔX . (f) Out-
291 lier result, presenting an increasing trend, which is likely to be due to an
292 insufficient number of points and a relatively small distance between them.

293 **Figure 4:** Histogram representing the distribution of the attenuation coefficient Z
294 for the 35 analyzed healthy subjects. A negative trend is clearly visible.
295 Please note that the two outliers ($Z=-91 \mu\text{m} \cdot \text{mm}^{-1}$ and $Z=17 \mu\text{m} \cdot \text{mm}^{-1}$,
296 respectively) correspond to cine-loops where only two measurement points
297 were available, thus leading to a potential estimation error.

Table 1: Average absolute error (err) of fitting between the measurement points and the linear regression model, as a function of the number of measurement points per cine-loops (N). Please note that the fitting error in those cine-loops with 2 measurement points is null by definition.

N	2	3	4	5	6	7
err (μm)	0 ± 0	22 ± 14	23 ± 25	47 ± 34	58 ± 44	70 ± 43

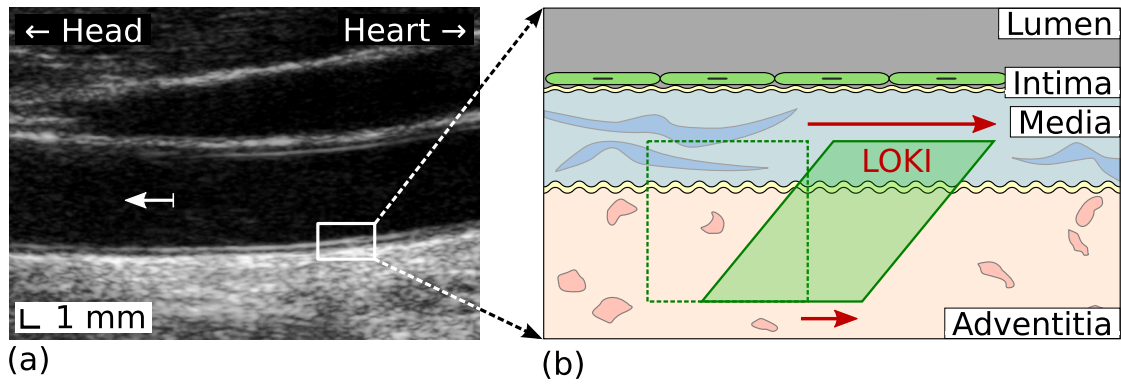


Figure 1: Common carotid artery (CCA). (a) Longitudinal B-mode ultrasound image of a healthy CCA *in vivo*. The direction of the blood flow in the lumen is indicated by the white arrow. (b) Illustration of the longitudinal kinetics (LOKI), occurring within the concentric layers of the wall during the heart beat.

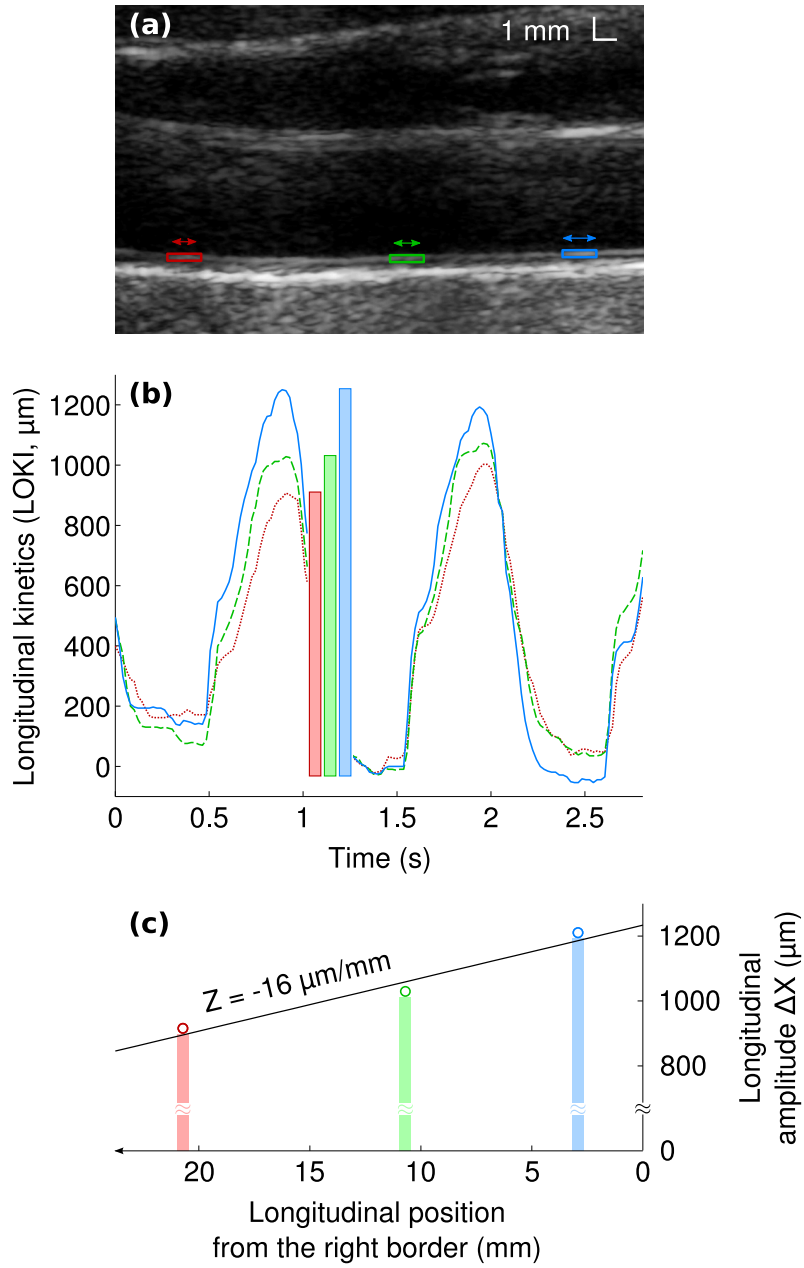


Figure 2: Example of LOKI amplitude ΔX , evaluated on a healthy subject. (a) Location of three regions of interest (ROIs), encompassing the tracked points within the intima-media complex of the far wall. The resulting LOKI amplitude ΔX during the cine-loop is represented by the double arrows. (b) Longitudinal component of the estimated trajectory, for the left (dotted red), middle (dashed green), and right (solid blue) tracked points. The peak-to-peak amplitude ΔX of each tracked point is represented by the vertical bar of the corresponding color. (c) Representation of the attenuation coefficient Z for this specific cine-loop, determined by linear regression (solid line) of the three tracked points (circles). For each tracked point, the x - and y -coordinates correspond to the abscissa of the ROI in (a), and to the estimated amplitude ΔX in (b), respectively.

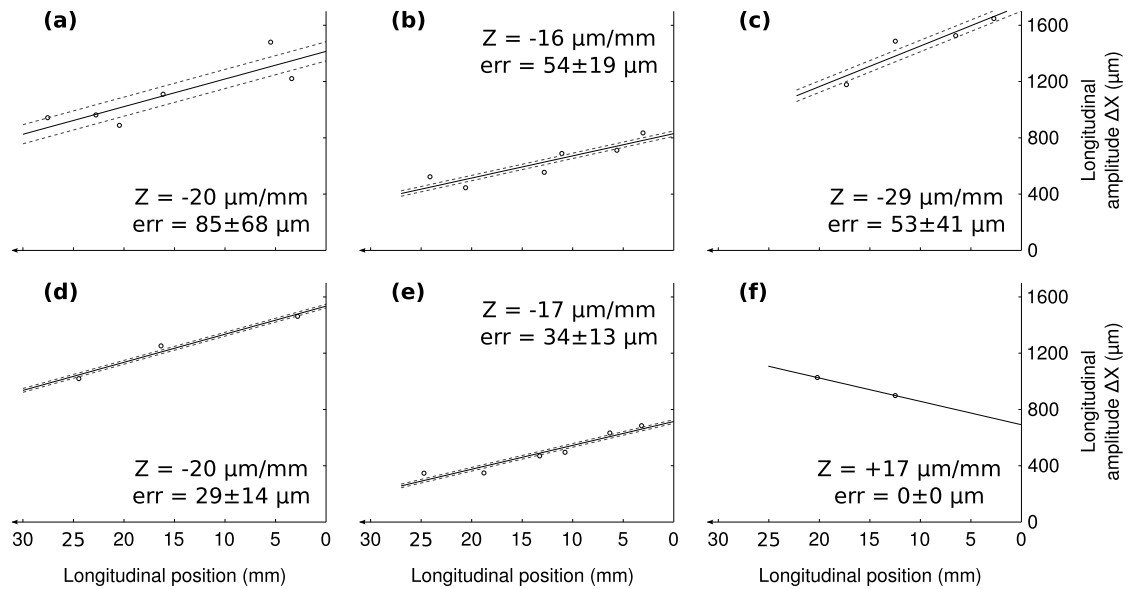


Figure 3: Examples of the attenuation coefficient Z in six participants, evaluated by means of linear regression (solid line) of the estimated LOKI amplitude ΔX (circles) over the length of the imaged region. The x -axis is oriented accordingly to the blood flow direction, from the right border of the image ($x = 0$) towards the left border. The fitting error (err) is indicated, and the corresponding standard deviation is represented by the dashed lines. (a-e) Representative examples of a progressive attenuation of ΔX . (f) Outlier result, presenting an increasing trend, which is likely to be due to an insufficient number of points and a relatively small distance between them.

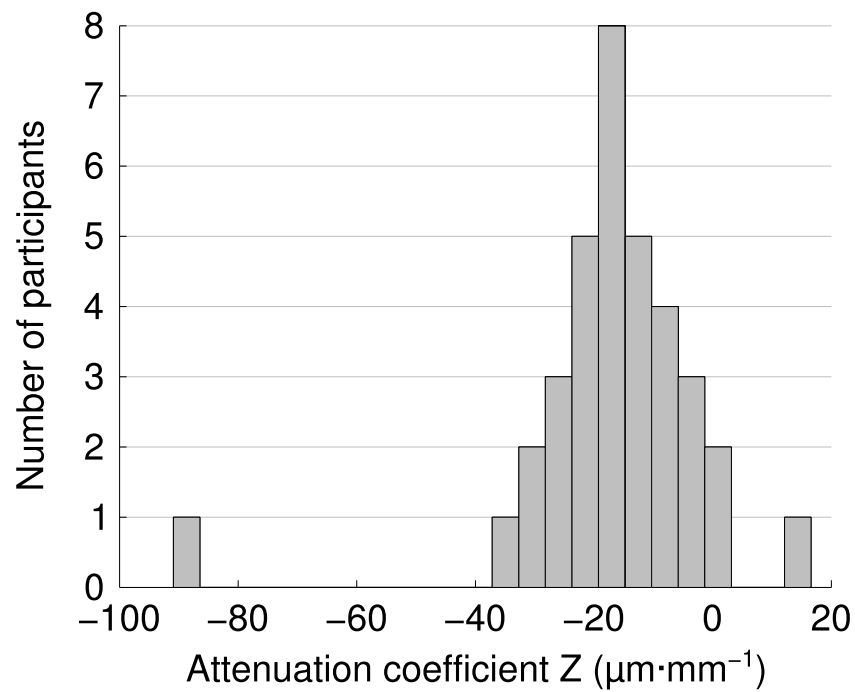


Figure 4: Histogram representing the distribution of the attenuation coefficient Z for the 35 analyzed healthy subjects. A negative trend is clearly visible. Please note that the two outliers ($Z=-91 \mu\text{m}\cdot\text{mm}^{-1}$ and $Z=17 \mu\text{m}\cdot\text{mm}^{-1}$, respectively) correspond to cine-loops where only two measurement points were available, thus leading to a potential estimation error.

298 **References**

- 299 Ahlgren ÅR, Cinthio M, Steen S, Nilsson T, Sjöberg T, Persson HW, Lindström
300 K. Longitudinal displacement and intramural shear strain of the porcine carotid
301 artery undergo profound changes in response to catecholamines. *American Jour-*
302 *nal of Physiology - Heart and Circulatory Physiology*, 2012;302:H1102–H1115.
- 303 Ahlgren ÅR, Cinthio M, Steen S, Persson HW, Sjöberg T, Lindström K. Effects
304 of adrenaline on longitudinal arterial wall movements and resulting intramu-
305 ral shear strain: a first report. *Clinical Physiology and Functional Imaging*,
306 2009;29:353–359.
- 307 Benetos A, Laurent S, Asmar RG, Lacolley P. Large artery stiffness in hyperten-
308 sion. *Journal of Hypertension*, 1997;15:S89–S97.
- 309 Chatzizisis YS, Coskun AU, Jonas M, Edelman ER, Feldman CL, Stone PH. Role
310 of endothelial shear stress in the natural history of coronary atherosclerosis and
311 vascular remodeling: Molecular, cellular, and vascular behavior. *Journal of the*
312 *American College of Cardiology*, 2007;49:2379–2393.
- 313 Cinthio M, Ahlgren ÅR, Bergkvist J, Jansson T, Persson HW, Lindström K. Lon-
314 gitudinal movements and resulting shear strain of the arterial wall. *American*
315 *Journal of Physiology*, 2006;291:H394–H402.
- 316 Cinthio M, Ahlgren ÅR, Jansson T, Eriksson A, Persson HW, Lindström K. Eval-
317 uation of an ultrasonic echo-tracking method for measurements of arterial wall
318 movements in two dimensions. *IEEE Transactions on Ultrasonics, Ferroelectrics,*
319 *and Frequency Control*, 2005;52:1300–1311.

- 320 Cunningham KS, Gotlieb AI. The role of shear stress in the pathogenesis of
321 atherosclerosis. *Laboratory investigation*, 2004;85:9–23.
- 322 Gastounioti A, Golemati S, Stoitsis J, Nikita KS. Comparison of Kalman-filter-
323 based approaches for block matching in arterial wall motion analysis from B-
324 mode ultrasound. *Measurement Science and Technology*, 2011;22:114008.
- 325 Gastounioti A, Golemati S, Stoitsis JS, Nikita KS. Carotid artery wall motion
326 analysis from B-mode ultrasound using adaptive block matching: in silico eval-
327 uation and in vivo application. *Physics in Medicine and Biology*, 2013;58:8647.
- 328 Golemati S, Stoitsis JS, Gastounioti A, Dimopoulos AC, Koropouli V, Nikita KS.
329 Comparison of block matching and differential methods for motion analysis of
330 the carotid artery wall from ultrasound images. *IEEE Transactions on Informa-
331 tion Technology in Biomedicine*, 2012;16:852–858.
- 332 Idzenga T, Hansen H, Lopata R, de Korte C. Estimation of longitudinal shear
333 strain in the carotid arterial wall using ultrasound radiofrequency data. *Ultra-
334 schall in der Medizin (Stuttgart, Germany: 1980)*, 2012a;33:E275–82.
- 335 Idzenga T, Holewijn S, Hansen HHG, de Korte CL. Estimating cyclic shear strain
336 in the common carotid artery using radiofrequency ultrasound. *Ultrasound in
337 Medicine & Biology*, 2012b;38:2229–2237.
- 338 Nichols WW, O’Rourke MF. McDonald’s blood flow in arteries: Theoretic, exper-
339 imental, and clinical principles. Fifth Edition. Oxford University Press, 2005.
- 340 Nilsson T, Ahlgren ÅR, Jansson T, Persson H, Nilsson J, Lindström K, Cinthio M.
341 A method to measure shear strain with high spatial resolution in the arterial wall

342 non-invasively in vivo by tracking zero-crossings of B-mode intensity gradients.
343 In: IEEE Ultrasonics Symposium, San Diego, California (USA), 2010. pp. 491–
344 494.

345 Persson M, Ahlgren ÅR, Jansson T, Eriksson A, Persson HW, Lindström K. A new
346 non-invasive ultrasonic method for simultaneous measurements of longitudinal
347 and radial arterial wall movements: first in vivo trial. *Clinical Physiology and*
348 *Functional Imaging*, 2003;23:247–251.

349 Rudski LG, Lai WW, Afilalo J, Hua L, Handschumacher MD, Chandrasekaran K,
350 Solomon SD, Louie EK, Schiller NB. Guidelines for the echocardiographic assess-
351 ment of the right heart in adults: A report from the american society of echocar-
352 diography. *Journal of the American Society of Echocardiography*, 2010;23:685–
353 713.

354 Soleimani E, Manijhe MD, Hajir S, Shahram SH, R. S. Kinematics parameter
355 extraction of longitudinal movement of common carotid arterial wall in healthy
356 and atherosclerotic subjects based on consecutive ultrasonic image processing.
357 *Physiology and Pharmacology*, 2012;16:165–178.

358 Svedlund S, Eklund C, Robertsson P, Lomsky M, Gan LM. Carotid artery lon-
359 gitudinal displacement predicts 1-year cardiovascular outcome in patients with
360 suspected coronary artery disease. *Arteriosclerosis, Thrombosis, and Vascular*
361 *Biology*, 2011;31:1668–1674.

362 Svedlund S, Gan L. Longitudinal common carotid artery wall motion is associated
363 with plaque burden in man and mouse. *Atherosclerosis*, 2011;217:120–124.

364 Tamborini G, Pepi M, Galli CA, Maltagliati A, Celeste F, Muratori M, Rezvanieh
365 S, Veglia F. Feasibility and accuracy of a routine echocardiographic assessment
366 of right ventricular function. *International journal of cardiology*, 2007;115:86–89.

367 WHO. World Health Organization, Cardiovascu-
368 lar diseases (CVDs), Fact sheet number 317.
369 <http://www.who.int/mediacentre/factsheets/fs317/en/index.html>,
370 2013.

371 Zahnd G, Boussel L, Marion A, Durand M, Moulin P, Sérusclat A, Vray D. Mea-
372 surement of two-dimensional movement parameters of the carotid artery wall
373 for early detection of arteriosclerosis: a preliminary clinical study. *Ultrasound*
374 *in Medicine & Biology*, 2011a;37:1421–1429.

375 Zahnd G, Boussel L, Sérusclat A, Vray D. Intramural shear strain can highlight
376 the presence of atherosclerosis: a clinical in vivo study. In: *IEEE Ultrasonics*
377 *Symposium*, Orlando, Florida (USA), 2011b. pp. 1770–1773.

378 Zahnd G, Orkisz M, Sérusclat A, Moulin P, Vray D. Evaluation of a Kalman-based
379 block matching method to assess the bi-dimensional motion of the carotid artery
380 wall in B-mode ultrasound sequences. *Medical Image Analysis*, 2013;17:573–585.

381 Zahnd G, Vray D, Sérusclat A, Alibay D, Bartold M, Brown A, Durand M,
382 Jamieson LM, Kapellas K, Maple-Brown LJ, O’Dea K, Moulin P, Celermajer DS,
383 Skilton MR. Longitudinal displacement of the carotid wall and cardiovascular
384 risk factors: associations with aging, adiposity, blood pressure and periodontal
385 disease independent of cross-sectional distensibility and intima-media thickness.
386 *Ultrasound in Medicine & Biology*, 2012;38:1705–1715.